Queuing Delay Analysis for Wavelength Routing Optical Satellite Networks Over Dual-Layer Constellation

Jingkai Yang, Qiwen Ran, and Jing Ma

***Abstract*—Optical satellite networks (OSN) utilizing wavelength division multiplexing (WDM) inter-satellite links (ISLs) and wavelength routing is becoming a new trend in constructing high-speed, large-capacity, and low-latency global network systems. Since the number of wavelength channels for the WDM ISLs is limited, the traffic requests might incur queuing delays due to the wavelength channel congestion. To evaluate the delay-tolerance characterization of dual-layer wavelength routing OSN (DWROSN), the ISLs arrival coefficient (IAC) is proposed to construct the queuing model. Simulation results are compared with theoretical results in terms of queuing length and queuing delays. The results show that the traffic intensity, number of wavelength channels, and node degree of the satellite have an impact on the queuing characterization of the DWROSN. The queuing model with the IAC can efficiently evaluate the queuing characterization of the DWROSN.**

***Index Terms*—Free-space optical (FSO) communication, optical satellite networks (OSN), wavelength routing, queuing delay.**

I. Introduction

FREE-SPACE optical (FSO) communications have drawn much attention for their unique advantages in many applications, such as high-speed data transmission, deep-space relay communications, mixed radio frequency/FSO communications, and so on [1], [2], [3]. Deploying optical communication terminals over hundreds of satellites and constructing optical satellite networks (OSN) is the key solution to build the future space-air-ground integrated networks [4], [5]. With the pointing, acquisition, and tracking (PAT) process, laser-based inter-satellite links (ISL) can be implemented among the satellite nodes, and the OSN can provide high-speed seamless coverage service for terrestrial users. Several commercial enterprises and national departments have announced their OSN plans, such as NeLS, Starlink, and EDRS.

Current designs of OSN are mainly based on laser ISLs and electronic onboard switching. The optical-electrical-optical processing of transit traffic is required at each intermediate satellite node, which causes processing delays and requires an additional onboard power supply. Therefore, the wavelength routing optical satellite networks (WROSN) by means of wavelength division multiplexing (WDM) ISLs and wavelength routing through onboard wavelength routers is proposed to solve this problem [6], [7]. Laser-based WDM ISLs provide multiple channels fitting the large bandwidth demand, and wavelength routing guarantees the routing process in the optical domain. This combination reduces the processing delay and power consumption at the intermediate satellite node, fitting the demand for reducing the transfer delay for traffic requests in WROSN.

Previous researches on WROSN mainly focus on link topology design of single-layer non-geosynchronous satellite constellations, such as NeLS and Iridium [8], and the goal is reducing the wavelength demand and improving the connectivity through link topology design [9] or routing and wavelength assignment (RWA) algorithm [10]. The main idea of these works is generating topology snapshots, and the ISLs switching is not considered. Focusing on dynamic topology, the RWA scheme based on a time-evolving graph is proposed to reduce the wavelength demand [11], but the traffic transmission delay is not considered. Though these works reduce the wavelength demand of the WROSN, it still needs hundreds of wavelengths for the WDM ISL to achieve full node-pair connectivity.

Since the number of wavelengths for the WDM ISLs can not meet the full connectivity demand, the traffic requests might incur queuing delays due to the wavelength channel congestion. Moreover, the over-topping time and the cache of the onboard processor are limited, therefore, it is necessary to evaluate the queuing characterization for the WROSN. Focus on queuing characterization, delay tolerance of intermittent satellite link based on time-limited $M/G/1$ queuing model is analyzed [12], but the link topology is too simple, which consists of two satellites and one ISL. For more complex link topology, the queuing model over non-geostationary satellite constellation is analyzed in [13], [14], but these works are not based on wavelength routing technology. For WROSN, the queuing delays are analyzed over a simplified NeLS constellation [15]. However, the queuing characteristics are obtained by numerical fitting and the link topology is stable, which means that the fitted results will no longer be applicable when the link topology is changed. So the queuing model for WROSN with dynamic changing topologies needs to be analyzed.

Manuscript received 31 January 2024; revised 21 March 2024; accepted 16 April 2024. Date of publication 19 April 2024; date of current version 2 May 2024. This work was supported by the Free-Space Optical Communication Technology Research Center. *(Corresponding author: Jingkai Yang.)*

The authors are with the National Key Laboratory of Science and Technology on Tunable Laser, Harbin Institute of Technology, Harbin 150001, China (e-mail: ynyxyjk@stu.hit.edu.cn; qiwenran@hit.edu.cn; majing@hit.edu.cn).

Digital Object Identifier 10.1109/JPHOT.2024.3391233

Deploying WROSN over the dual-layer geosynchronous (GEO) and low Earth orbit (LEO) constellation is a new trend for future satellite communication networks. Compared with single-layer non-geosynchronous constellations, the GEO satellites could provide stable access for terrestrial users, and the dual-layer constellation could provide better terrestrial coverage and reduce the long multi-hops relay services. Constructing a queuing model for dual-layer WROSN (DWROSN) could provide a reference for evaluating network performance, such as queuing length and queuing delays. Queuing length represents the cached traffic requests in the network, which corresponds to the cache size of the onboard processors. Queuing delay has a key impact on the quality of service for traffic transmission. Therefore, the study of the queuing model for the DWROSN can provide a reference for evaluating the traffic intensity threshold for traffic requests in the network. However, the link topologies for the dual-layer constellation are dynamically changing, and this characteristic should be considered in construing the queuing model.

Focusing on the above topics, the theoretical model of queuing characterization for the DWROSN with dynamic link topology is proposed and analyzed in this paper. The contribution of this paper is three-fold: i) We have created a dual-layer satellite constellation, and proposed the mathematical model of the visibility of the ISLs; ii) The ISLs arrival coefficient is proposed to construct the queuing system based on Kendall $M/M/m$ model for DWROSN, and the expressions of the queuing delay and queuing length have been obtained. iii) The dynamic topologies with randomly connected ISLs have been established. At the same time, the traffic requests based on the Markov chain have been adopted into the DWROSN, and the simulation results have been compared with theoretical results in terms of queuing length and queuing delay.

The rest of this paper is organized as follows. Section II introduces the model of the DWROSN, at the same time, the mathematical model of the ISLs visibility is given. Section III proposes the queuing model for the DWROSN. Section IV gives the simulations and analysis. Finally Section V concludes this work.

II. Establishment of the Dynamic Topologies

In this paper, the WROSN is deployed on a dual-layer constellation, which consists of two Walker-Star constellations. The diagram is shown in Fig. 1. The Walker constellation can be described by five parameters [16]: $T/P/F : h : I$, which means the constellation contains T satellites. These satellites are evenly distributed in P circular orbits, and the orbital altitude and inclination are h and I, respectively. F represents the inter-plane spacing factor. Subscripts L and G are used to distinguish the parameters belonging to the LEO and GEO layer constellation, respectively. The LEO layer Walker-Star constellation can be denoted as $T_L/P_L/F_L : h_L : I_L = 66/6/1 : 780 : 86.4$, and the GEO layer Walker-Star constellation can be denoted as $T_G/P_G/F_G : h_G : I_G = 3/1/0 : 35786 : 0$. The primary parameters of the DWROSN are shown in Table I. The node degree represents the number of LCTs onboard the satellite.

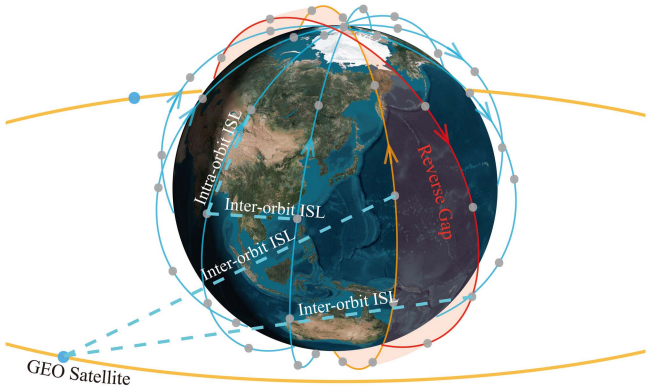

Fig. 1. Diagram of dual-layer constellation and ISL.

TABLE I
Primary Parameters of the DWROSN

Parameters	LEO layer	GEO layer
Orbit inclination (I)	86.4°	0°
Orbit altitude (h)	780 km	35786 km
Orbit period (U)	6027 s	86400 s
Number of orbits (P)	6	1
Number of satellites per orbit (Q)	11	3
Node degree($\mathcal{D}$)	$4 \sim 6$	$4 \sim 6$
Inter plane spacing (F)	1	-

A. Visibility Determination for the Node-Pairs

The topology for the DWROSN consists of the satellite nodes and the ISLs established among the satellite nodes. Since the visibility of most of the node-pairs is impermanent, the topology dynamically changes as the establishment and disconnection of the ISLs. The satellite trajectory can be predicted in advance, so the visibility versus time for all node-pairs in the WROSN can be predicted and the topologies versus time can be determined in advance. For a satellite $S_{l,pq}$, which represents the q-th satellite in the p-th orbital plane of l layer constellation, the location vector $\boldsymbol{r}_{l,pq}(\boldsymbol{x}_{l,pq}(t), \boldsymbol{y}_{l,pq}(t), \boldsymbol{z}_{l,pq}(t))$ can be denoted as

$$\begin{aligned}\boldsymbol{x}_{l,pq}(t) = &\left[R_l \cos\Omega_{l,p} \cos\left(\omega_l t + \Phi_{l,q} + \Delta u_{l,q}\right)\right. \\ &\left. - R_l \cos I_l \sin\Omega_{l,p} \sin\left(\omega_l t + \Phi_{l,q} + \Delta u_{l,q}\right)\right] \hat{\boldsymbol{i}}\end{aligned} \tag{1}$$

$$\begin{aligned}\boldsymbol{y}_{l,pq}(t) = &\left[R_l \sin\Omega_{l,p} \cos\left(\omega_l t + \Phi_{l,q} + \Delta u_{l,q}\right)\right. \\ &\left. + R_l \cos I_l \cos\Omega_{l,p} \sin\left(\omega_l t + \Phi_{l,q} + \Delta u_{l,q}\right)\right] \hat{\boldsymbol{j}}\end{aligned} \tag{2}$$

$$\boldsymbol{z}_{l,pq}(t) = R_l \sin I_l \sin\left(\omega_l t + \Phi_{l,q} + \Delta u_{l,q}\right) \hat{\boldsymbol{k}} \tag{3}$$

where $\hat{\boldsymbol{i}}, \hat{\boldsymbol{j}}, \hat{\boldsymbol{k}}$ represent the unit vectors of the X, Y and Z axis, respectively. Under the ECI coordinate system, the X-axis is aligned with the equinox of the Earth. The Z-axis is aligned with the rotation axis of the Earth. The Y-axis is rotated by 90° East about the celestial equator. R_l and ω_l represent the orbital radius and angular velocity of the l layer constellation, respectively. $p, q \in \mathbb{Z}$. For LEO layer constellation, $0 \leqslant p \leqslant P_L - 1$, $0 \leqslant$

$q \leqslant Q_L - 1$, and $Q_L = T_L/P_L$. For GEO layer constellation, $0 \leqslant p \leqslant P_G - 1$, $0 \leqslant q \leqslant Q_G - 1$, and $Q_G = T_G/P_G$.

$\Phi_{l,q} + \Delta u_{l,q}$ and $\Omega_{l,p}$ represents the phase angle and the right ascension of ascending node for the q-th satellite in p-th orbital plane of l layer constellation, respectively. And these parameters can be denoted as

$$\Omega_{l,p} = \begin{cases} \pi p_l/P_l, & \text{Walker} - \text{Star} \\ 2\pi p_l/P_l, & \text{Walker} - \text{Delta} \end{cases} \tag{4}$$

$$\Phi_{l,q} = \frac{2\pi q_l}{Q_l} \tag{5}$$

$$\Delta u_{l,q} = \frac{2\pi q_l F_l}{T_l} \tag{6}$$

From (1),(2),(3),(4),(5),(6), the location vectors versus time for all satellites in the DWROSN can be determined. Then the visibility between satellite $S_{l,pq}$ and $S_{l',p'q'}$ versus time can be obtained as

$$\begin{cases} (\boldsymbol{r}_{l,pq}(t) - \boldsymbol{r'}_{l',p'q'}(t)) \cap \mathcal{O}_{\text{Earth}} = \emptyset, & \text{visible} \\ (\boldsymbol{r}_{l,pq}(t) - \boldsymbol{r'}_{l',p'q'}(t)) \cap \mathcal{O}_{\text{Earth}} \neq \emptyset, & \text{invisible} \end{cases} \tag{7}$$

where $\mathcal{O}_{\text{Earth}}$ represents the sphere of the Earth, and $(\boldsymbol{r}_{l,pq}(t) - \boldsymbol{r'}_{l',p'q'}(t))$ represents the location vector of the ISL between $S_{l,pq}$ and $S_{l',p'q'}$.

Based on the mathematical model obtained above, the visibility versus time of all node-pairs in the DWROSN can be predicted, and the potential ISLs set can be determined. The links assignment scheme selects the ISLs from the potential ISLs set and establishes the topology for the DWROSN. To guarantee the stability of the topology and reduce link switching, the duration of the ISLs between the node-pairs must be considered. Besides, the relative motion between the satellites in different orbital planes is another impact in selecting the potential ISLs, especially for the node-pairs near the polar region and between the reverse gap. The high relative angular velocity of these node-pairs brings high Doppler shift [17] and also makes it difficult to maintain the connecting of the ISLs. Therefore, the ISLs between the node-pairs in the area above 70° north and south latitude and the node-pairs between the reverse gap are not considered the potential ISLs.

B. Topology Initialization for the DWROSN

In this paper, the dynamic topologies are established following the links assignment scheme based on the arbitrarily connected algorithm [18], [19]. Each ISL occupies one LCT on each side, and only one ISL can be established between each node-pair. The topology of the DWROSN at $t = 0\ s$ is initialized following two steps:

1) Determination for the Potential ISLs Set: Determine the visibility for all node-pairs in the DWROSN through (7). Then select the ISLs, whose duration is not less than the duration limitation, as the potential ISLs set. At the same time, the satellites at both sides of these potential ISLs are not in the polar latitude area or the orbital planes between the reverse gap.

2) ISLs Establishment: Randomly select an ISL from the potential ISLs set and attempt to establish this selected ISL. A new ISL can be established only if there exists at least one idle LCT on both its interconnecting sides. Repeat this step until all LCTs are occupied or all potential ISLs have been attempted.

C. ISLs Switching Rule

As the operation time goes on, the impermanent ISLs will be disconnected and new ISLs will be established. In this paper, the ISLs switching scheme is also based on the arbitrarily connected algorithm. The switching process at operation time t works following three steps:

1) Disconnection of the ISLs: Check the remaining time of all connected ISLs, and disconnect the ISLs whose remaining time is zero.

2) Determination for the Potential ISLs Set: Determine the visibility for all node-pairs in the DWROSN and establish the potential ISLs set at time t. Then eliminate the potential ISLs, whose interconnecting nodes do not exist idle LCT, from the potential ISLs set.

3) Establishment of New ISLs: Randomly select an ISL from the potential ISLs set and attempt to establish this selected ISL. Repeat this step until all LCTs are occupied or all potential ISLs have been attempted.

LCTs will not be fully occupied due to the limitations of the polar region, reverse gap, and visibility duration. The LCTs utilization, α, is proposed to describe the percentage of active LCTs in the DWROSN. α is defined as the ratio of active LCTs to all LCTs in the DWROSN, which can be denoted as

$$\alpha = \frac{1}{N} \sum_{i=1}^{N} \frac{d_i}{\mathcal{D}_i} \tag{8}$$

where N represents the number of satellites in the dual-layer constellation. d_i and $\mathcal{D}_i$ represent the number of occupied LCTs and the node degree of i-th satellite in the DWROSN, respectively.

Once an ISL has been established, the corresponding node-pair is connectable, and the traffic request between this node-pair can be directly transited. While the destination node is one ISL away from the source node, a consecutive light path with the same wavelength channel is arranged through several intermediate nodes, and this node-pair is connectable through the wavelength routing service. The node-pair connectivity, β, is proposed to describe the percentage of connectable node-pairs within the maximum allowable hop count to all node-pairs, which can be denoted as

$$\beta = \left. \frac{2N_p}{N(N-1)} \right|_{\{N_{hops}\}_{\max}} \tag{9}$$

where $\{N_{hops}\}_{\max}$ represents the maximum allowable hops count, and N_p represents the number of connectable node-pairs within the maximum allowable hops.

III. Queuing Model for DWROSN

Since the number of wavelength channels for the WDM ISLs is limited, the traffic requests might incur queuing delays due to the wavelength channel congestion. The diagram of the queuing model for the DWROSN is shown in Fig. 2. Each WDM ISL

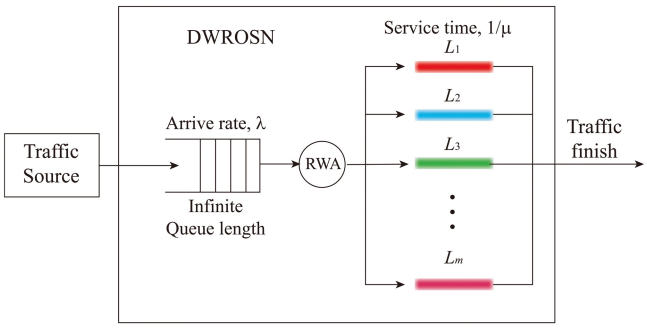

Fig. 2. Diagram of $M/M/m$ queuing model for DWROSN.

in the DWROSN has m wavelength channels, which means that at most m traffic requests can be transmitted simultaneously on the same ISL. Assume that the arrived traffic requests among the node-pairs in the DWROSN are Poisson flows, and the arrival interval and service duration of the traffic requests are with negative exponential distribution. The mean arrival rate and mean service duration of the traffic requests are λ and $1/\mu$, respectively. Thus the traffic intensity for the DWROSN is $\rho = \lambda/\mu$.

For each traffic request, the route path is determined by the RWA algorithm, and each route path will occupy one wavelength channel on one ISL or the same wavelength channel on several consistent ISLs. The corresponding ISLs occupied by the traffic request could remain connected until the transportation finishes. Queuing occurs only when at least one ISL of the route path, which will be used by the newly arrived traffic request, conflicts with the ISLs already occupying other traffic requests in the DWROSN. The study of the queuing characterization for DWROSN transfers to the study of the queuing characterization for an ISL l in the DWROSN. Let $P_{l,k}(t_1, t_2)$ represent the probability of the number of the traffic requests arrived in $[t_1, t_2]$, and the route paths of these traffic requests all occupy the same ISL l. $k \in \mathbb{N}$. During a short time slot $[t, t + \Delta t]$, the probability that one traffic request arrives is given by

$$P_{l,1}(t, t + \Delta t) = \lambda P_l \Delta t + o(\Delta t) \tag{10}$$

where P_l is the ISL arrival coefficient (IAC), representing the probability of the route path of the traffic request occupying ISL l. IAC is determined by the RWA algorithm and the topology of the DWROSN. Suppose the traffic requests are equally distributed among the node-pairs in the DWROSN, then P_l can be denoted as

$$P_l = \frac{\sum_{\substack{i,j=1 \\ i \neq j}}^{N} \boldsymbol{hops}(S_i, S_j) T_{ij}}{\sum_{i=1}^{N} d_i} \frac{1}{\eta} = \frac{P_T}{\eta} \tag{11}$$

where $\boldsymbol{hops}(S_i, S_j)$ represents the relay hop count between a source-destination node-pair S_i and S_j, which is determined by the RWA algorithm together with the link topology. T_{ij} represents the distribution of the traffic request between the node-pair, which is determined by the traffic requests flow. So $\sum \boldsymbol{hops}(S_i, S_j) T_{ij}$ represents the mathematical expectation of the number of ISLs needed for transiting a newly arrived traffic request in the DWROSN. d_i is the number of the occupied LCTs in S_i. Since not all of the ISLs and their wavelength channels can be utilized at the same time, the maximum utilization of the ISLs, η, is proposed to represent the maximum ratio of the number of occupied wavelength channels to all wavelength channels for the WDM ISL during the operation time, while the queuing system of the DWROSN is within the steady state. Topology coefficient P_T is proposed to represent the value of the ηP_l. Since the route paths of the traffic request in the DWROSN are determined by the RWA algorithm based on the link topology and the number of connected ISLs is a characteristic parameter of the link topology, the IAC represents the link topology characteristics of the DWROSN. Once the topology of the DWROSN, RWA algorithm, and traffic requests distribution are determined, P_l can be determined, which represents the probability that an arriving traffic request is routed using ISL l. Since the queuing list is of infinite length, the signature that the queuing system is within the steady state is that the queuing length converges to a constant value after a long operation time.

Divide a finite time interval t into n short time slots, $t = n\Delta t$. The k traffic requests that arrived during t are arbitrarily distributed at k time slots. From the binomial distribution, the probability of k traffic requests arrived at the ISL l can be obtained as

$$\begin{aligned} P_{l,k}(t) &= \lim_{n \to \infty} C_n^k (P_{l,1}(t))^k (1 - P_{l,1}(t))^{n-k} \\ &= \frac{(\lambda_l t)^k}{k!} e^{-\lambda_l t} \end{aligned} \tag{12}$$

where $\lambda_l = \lambda P_l$ represents the arrival rate of the traffic requests at ISL l. So the traffic requests that arrive at ISL l are Poisson flows, and the arrival interval and service duration of the traffic requests are with negative exponential distribution. The mean service duration is $1/\mu$.

There are m wavelength channels for each WDM ISL. When a traffic request arrives queuing system of the DWROSN at t, the RWA scheme determines the route path and the wavelength channel for the traffic request. If the RWA is successful, this traffic request will leave the queuing system after its service duration. If the RWA is unsuccessful due to the wavelength channel congestion, this traffic request will join the queuing list and wait for the next routing arrangement. The queuing list is of infinite length, and the traffic requests in the queuing list are served in the order of first-arrived first-served.

When the queuing system has operated for a long time, if the traffic intensity is lower than the threshold, the queuing system enters a steady state, at which point the probabilities of the state as well as other queuing characteristics will be independent of time. To evaluate the queuing characterization of the DWROSN, the state transition diagram of the WMD ISL in the DWROSN is shown in Fig. 3. Let p_i represent the probability of i-th sate for the ISL in the DWROSN, $i \in \mathbb{N}$. The value of p_i represents the probability that there are i traffic requests transmitting on the ISL. The arcs with arrows in the figure indicate that the queuing system can transfer from the source state to the destination state, and the values on the arcs indicate the instantaneous transfer rate of the state. Since the queuing system allows infinite queuing

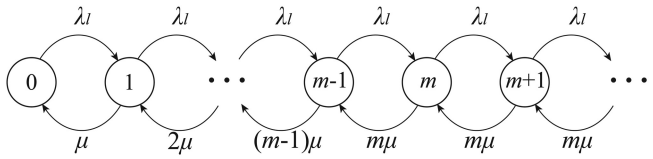

Fig. 3. State transition diagram of the WDM ISL.

length, the instantaneous transfer rates from state i to $i+1$ are all λ_l, which indicates that the probability of adding a traffic request during a time interval Δt is $\lambda_l \Delta t$. When $i \leqslant m$, since the WDM ISL has m wavelength channels, the instantaneous transfer rates from state i to $i-1$ is $i\mu$, which indicates that the probability of a traffic request completes the service during a time interval Δt is $i\mu\Delta t$. When $i \geqslant m+1$, the new arriving traffic request will experience queuing delay due to wavelength channel congestion, then the instantaneous transfer rates from state i to $i-1$ is always $m\mu$, which indicates that the probability of a traffic request completes the service during a time interval Δt is $m\mu\Delta t$. Then the state transition equations are obtained as

$$\begin{cases} \lambda_l p_0 & = \mu p_1 \\ (\lambda_l + i\mu)\, p_i & = \lambda_l p_{i-1} + (i+1)\,\mu p_{i+1}, \quad 1 \leqslant i \leqslant m-1 \\ (\lambda_l + m\mu)\, p_i & = \lambda_l p_{i-1} + m\mu p_{i+1}, \quad i \geqslant m \end{cases} \tag{13}$$

Let $\rho_l = \lambda_l/(m\mu)$ represent the traffic intensity at the ISL l. Since the queuing system is within the steady state, it requires $\rho_l \leqslant 1$. Substituting ρ_l into (13), the probability of the i-th state can be obtained as

$$p_i = \begin{cases} \frac{m^i \rho_l^{\,i}}{i!} p_0, & 1 \leqslant i \leqslant m-1 \\ \frac{m^m \rho_l^{\,i}}{m!} p_0, & i \geqslant m \end{cases} \tag{14}$$

According to the probability normalization condition, the sum of the probabilities that the queuing system is in each state is 1, which means that the sum of p_i is 1. Then we have

$$\begin{aligned} 1 \equiv \sum_{i=0}^{\infty} p_i &= \left[\sum_{i=0}^{m-1} \frac{m^i {\rho_l}^i}{i!} + \sum_{i=m}^{\infty} \frac{m^m {\rho_l}^i}{m!} \right] p_0 \\ &= \left[\sum_{i=0}^{m-1} \frac{m^i {\rho_l}^i}{i!} + \frac{m^m}{m!} {\rho_l}^m \frac{1}{(1-\rho_l)} \right] p_0 \end{aligned} \tag{15}$$

From (15), the initial state of the queuing system can be obtained as

$$p_0 = \left(\sum_{k=0}^{m-1} \frac{1}{k!} (m\rho_l)^k + \frac{(m\rho_l)^m}{m!\,(1-\rho_l)} \right)^{-1} \tag{16}$$

Then the average queuing length of the traffic requests in the DWROSN, L_q, is obtained as

$$\begin{aligned} L_q &= \sum_{i=m+1}^{\infty} (i-m) p_i \\ &= \frac{\rho_l^m \lambda_l \mu}{(m-1)!(m\mu - \lambda_l)^2} p_0 \end{aligned} \tag{17}$$

Since the queuing list is of infinite length, so the effective arrival rate of the traffic requests is always λ_l. According to the Little's theorem, the average queuing delay is obtained as

$$\begin{aligned} D_q &= \frac{L_q}{\lambda_l} \\ &= \frac{\rho_l^m \mu}{(m-1)!(m\mu - \lambda_l)^2} p_0 \end{aligned} \tag{18}$$

IV. Numerical Results and Analysis

To investigate the queuing characterization of the DWROSN and compare it with the queuing model proposed above, the traffic transportation is simulated over the DWROSN. The primary parameters of the DWROSN are based on Table I. The traffic requests with different traffic intensities are generated in advance, and the arrival rate and service duration of the traffic requests are with a negative exponential distribution. The mean arrival interval is set to 2 s. The sources and destinations of the traffic requests are distributed equally among all node-pairs in the dual-layer constellation. The route paths of the traffic requests are determined by Dijkstra's algorithm, and the wavelength channels are assigned following the First-fit scheme.

At the beginning of the simulation, the topology of the DWROSN is constructed following the initializing procedure proposed in Section II. The duration limitation of the potential ISLs is set to 900 s. Since the ISLs are randomly connected, to ensure the topologies are identical at the beginning of the simulation, 100 topologies are generated in advance for each node degree, and the topology with the smallest P_T is selected as the initial topology of the DWROSN. As the operation time goes on, the topology changes with the disconnection and establishment of the ISLs following the switching rule proposed in Section II, and the switching procedure will operate every second in the simulation. The operation time of the simulation is $0 \sim 10000$ s. The traffic requests with different traffic intensities are simulated 10 times in the DWROSN with different wavelength channels and node degrees.

Fig. 4 shows the average LCT utilization versus time of the DWROSN with different node degrees. The lines in the figure give the average value of the LCT utilization, and the colored areas give the range of the variation of the LCT utilization. The average values of the LCT utilization are 0.83, 0.79, and 0.75 for the node degrees are 4, 5, and 6, respectively. Considering the ISL restriction on the areas of the polar region and reverse gap, the topologies of the DWROSN constructed following the arbitrarily connected algorithm still have high LCT utilization.

Fig. 5 shows the topology coefficient of the DWROSN versus time with different node degrees. The colored areas give the range of the variation of the topology coefficient. The average values of the topology coefficient are 0.038, 0.028, and 0.023 for the node degrees of the DWROSN are 4, 5, and 6, respectively. As the node degree increases, the topology coefficient of the DWROSN decreases. More node degrees of the DWROSN means more ISLs can be established among the satellites. The traffic request has more alternative route paths to be selected by the RWA algorithm, and the probability of a link being occupied decreases.

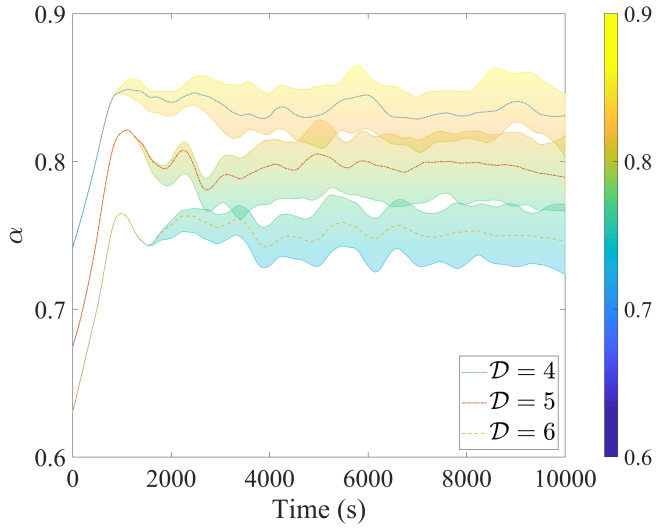

Fig. 4. Average LCT utilization versus time of the DWROSN with different node degrees.

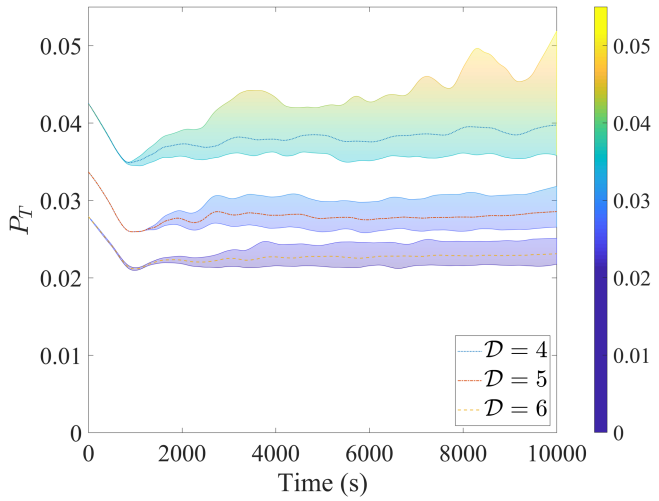

Fig. 5. Topology coefficient of the DWROSN versus time with different node degrees.

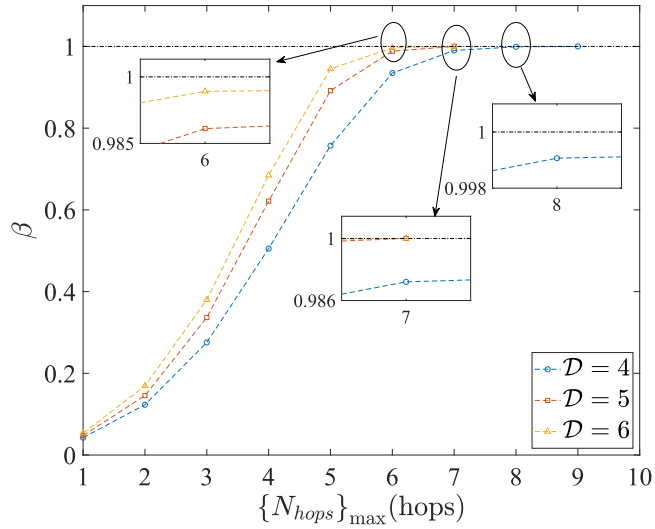

Fig. 6. Node-pair connectivity of the DWROSN with different node degrees at $t = 0\ s$.

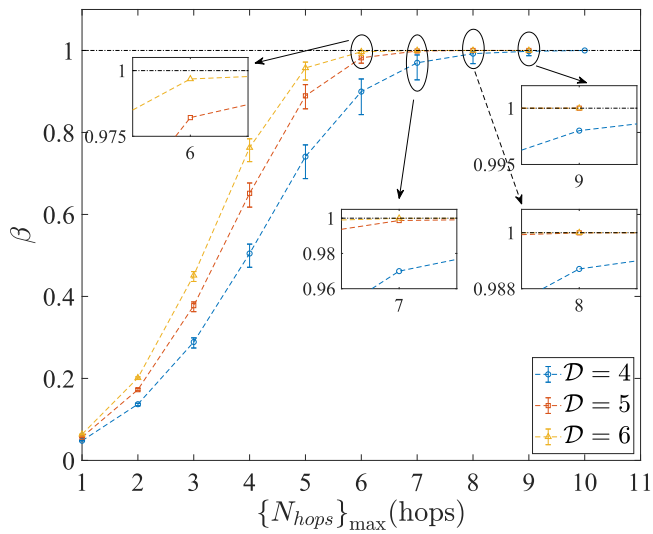

Fig. 7. Average node-pair connectivity of the DWROSN with different node degrees during the operation time.

Fig. 6 shows the relationship between the node-pair connectivity and the maximum allowable hop for the DWROSN with different node degrees at $t = 0$ s. As the maximum allowable hop increases, the node-pair connectivity of the DWROSN increases. The DWROSN with 4 node degree needs 9 hops to achieve the full node-pair connectivity, while the DWROSN with 5 and 6 node degrees requires 7 hops. Considering the traffic requests are equally distributed among all node-pairs in the DWROSN, the average relay hop counts for the traffic request are 4.37, 3.97, and 3.77 hops for the node degrees of the DWROSN are 4, 5, and 6, respectively. Under the same maximum allowable relay hop count, the DWROSN with higher node degree has a better node-pair connectivity.

As the operation time goes on, the topologies change with the disconnection and establishment of the ISLs. Fig. 7 shows the average node-pair connectivity of the DWROSN under different maximum allowable relay hop counts with different node degrees. The points in the figure represent the average value of the node-pair connectivity of the DWROSN, and the error bars give the standard errors of the node-pair connectivity. Since the ISLs are randomly connected based on the arbitrary switching scheme, there exist some node-pairs that require long relay hops to achieve connectivity. The DWROSN with the high node degree requires less relay hop count to achieve the full node-pair connectivity than with the low node degrees. The average relay hop counts are 4.42, 3.87, and 3.57 hops for the node degree of the DWROSN are 4, 5, and 6, respectively. From increasing the number of onboard LCTs, the average relay hop count of the node-pairs decreases, which means that the traffic request transiting in the DWROSN with the high node degree requires fewer relay hops.

Fig. 8 shows the average queuing length of the DWROSN with different n_λ under different traffic intensities. The node

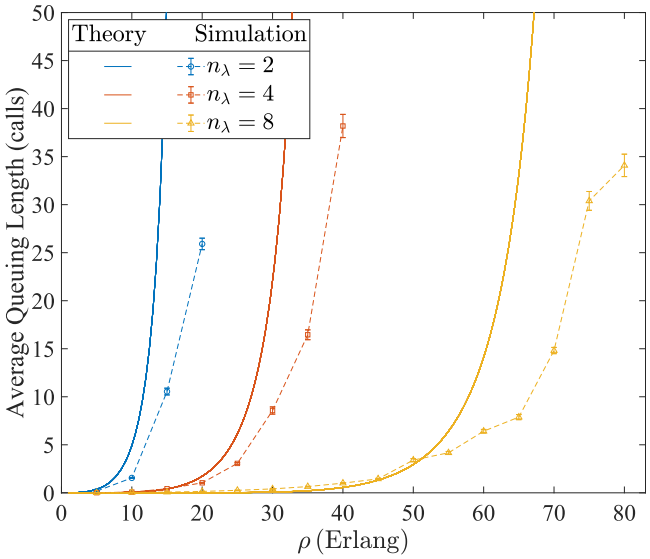

Fig. 8. Average queuing length of the DWROSN with different n_λ under different traffic intensities.

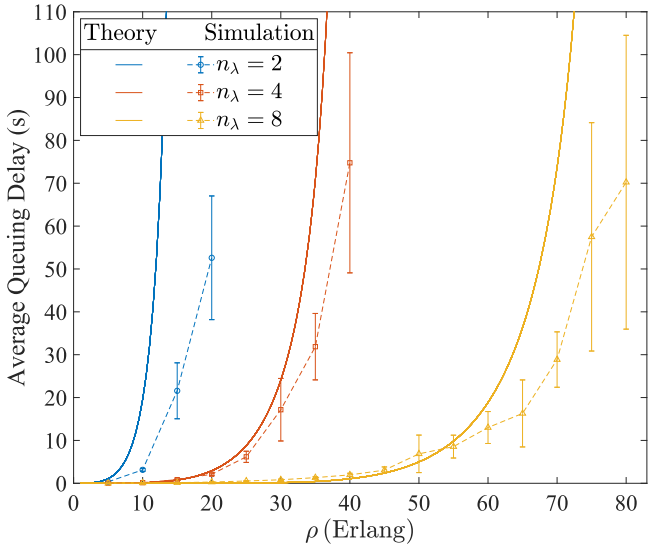

Fig. 9. Average queuing delay of the DWROSN with different n_λ under different traffic intensities.

degree of the DWROSN in the figure is 4. n_λ is the number of the wavelength channels. Since the state of the queuing system at the beginning of the simulation is not steady state, the simulation results of queuing length and queuing delays in the rest of this paper are statistical averages for traffic requests arrived during $[4000, 7000)$s. The lines in the figure represent the theoretical results, and the points represent the simulation results. The error bars in the figure represent the standard error for the corresponding simulated results. Within the steady state, the average queuing length of the DWROSN converges to a constant value after a period of operation time. The maximum traffic intensities are 20, 40, and 80 corresponding to the number of wavelength channels of the DWROSN are 2, 4, and 8, respectively. The average maximum utilization of the ISLs is 0.39. As can be seen from the figure, increasing the number of wavelength channels reduces the average queuing length of the DWROSN with the same traffic intensity. At low traffic intensities, the queuing length converges to a constant value within the operation time, and the theoretical results match well with the simulated results. The average queuing lengths are less than 5 calls for the number of wavelength channels of the DWROSN are 2, 4, and 8 and corresponding traffic intensities are 10, 25, and 55, respectively. The queuing length grows exponentially as the traffic intensity increases. The theoretical results tend to infinity when the traffic intensity tends to the maximum value allowed within the steady state of the DWROSN. At low traffic intensities, the queuing system can enter the steady state within the operation time, so the simulation results fit well with the theoretical results. At high traffic intensities, the queuing system needs more operation time to enter the steady state. As the traffic intensity approaches the threshold value that the queuing system can carry, the required operation time will tend to be infinite, and the theoretical results of the queuing length tend to be infinite. However, due to the operation time constraints, the number of traffic requests that arrive during the operation time is finite. Therefore, at high traffic intensities, the simulation results of the queuing length are less than the theoretical results.

Fig. 9 shows the average queuing delay of the DWROSN with different numbers of wavelength channels under different traffic intensities. The node degree in this figure is 4. At low traffic intensities, the theoretical results match well with the simulated results. The average queuing delays are less than 10 s for the DWROSN with 2, 4, and 8 channels and the corresponding traffic intensities are 10, 25, and 55, respectively. The queuing delay grows exponentially as the traffic intensity increases. The theoretical results tend to infinity when the traffic intensity tends to the maximum value allowed within the steady state of the DWROSN. At high traffic intensities, the simulation results are lower than the theoretical results. At high traffic intensities, the traffic requests that require long relay hops make it difficult to achieve successful route service. At the end of the simulation, these traffic requests still have not been served, so the simulated queuing delays are lower than their actual queuing delays. As can be seen from the figure, increasing the number of wavelength channels reduces the average queuing delay of the DWROSN with the same traffic intensity. Therefore, increasing the number of wavelength channels for the WDM ISLs is a method to improve the traffic transition quality.

Besides the number of wavelength channels, the node degree has an impact on the queuing characterization of the DWROSN. Fig. 10 shows the average queuing length of the DWROSN with different node degrees under different traffic intensities. The number of wavelength channels in this figure is 4. The maximum traffic intensities are 40, 60, and 80 corresponding to the node degrees of the DWROSN are 4, 5, and 6, respectively. As the node degree increases, the average maximum utilization of ISLs increases. The average maximum utilization of the ISLs is 0.39, 0.46, and 0.47, respectively. As traffic intensities increase, the queuing length of the DWROSN increases exponentially. Under

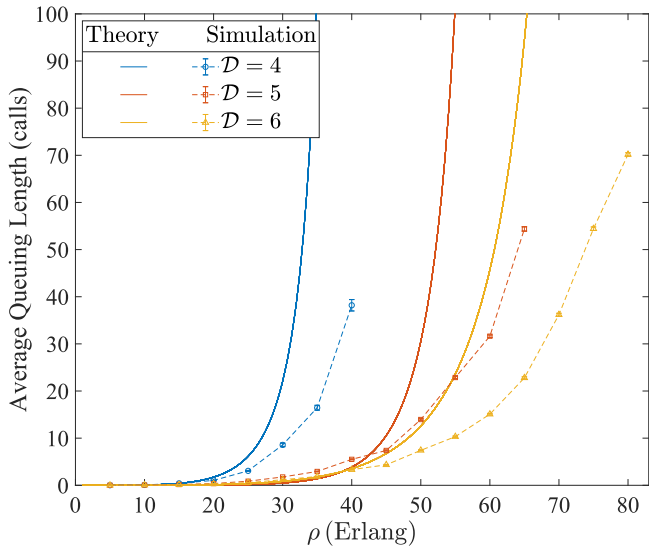

Fig. 10. Average queuing length of the DWROSN with different node degrees under different traffic intensities.

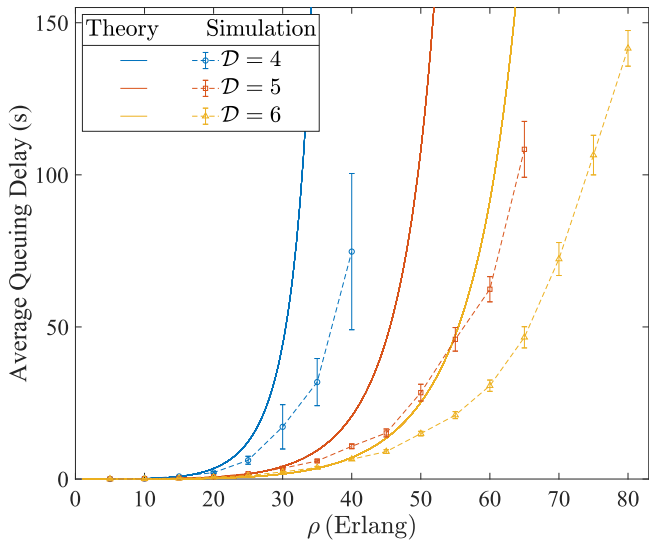

Fig. 11. Average queuing delay of the DWROSN with different node degrees under different traffic intensities.

the same traffic intensity, increasing the node degrees reduces the average queuing length of the DWROSN. Therefore, increasing the number of onboard LCTs can achieve the goal that transiting more traffic requests with the same onboard cache size.

Fig. 11 shows the average queuing delay of the DWROSN with different node degrees under different traffic intensities. As traffic intensities increase, the queuing delay of the DWROSN increases exponentially. Under the same traffic intensity, increasing the node degrees reduces the average queuing delay of the DWROSN. Therefore, besides increasing the wavelength channels, increasing the number of onboard LCTs is another method to improve the traffic transition quality.

V. Conclusion

In this paper, the characteristic of the traffic requests arriving in ISL is analyzed based on the proposed ISLs arrival coefficient, and the queuing model based on the ISLs arrival coefficient is proposed and analyzed over the DWROSN with dynamic link topologies. The equations of the queuing length and queuing delay within the steady state have been obtained. Under different conditions, the simulation results match well with the theoretical results. The proposed queuing model provides significant insight into the WROSN deployment, such as the impacts of the number of onboard LCTs, number of wavelength channels, and allowable traffic intensity.

References

[1] G. Xu, Q. Zhang, Z. Song, and B. Ai, "Relay-assisted deep space optical communication system over coronal fading channels," *IEEE Trans. Aerosp. Electron. Syst.*, vol. 59, no. 6, pp. 8297–8312, Dec. 2023.

[2] V. W. S. Chan, "Free-space optical communications," *J. Lightw. Technol.*, vol. 24, no. 12, pp. 4750–4762, Dec. 2006.

[3] G. Xu and Q. Zhang, "Mixed RF/FSO deep space communication system under solar scintillation effect," *IEEE Trans. Aerosp. Electron. Syst.*, vol. 57, no. 5, pp. 3237–3251, Oct. 2021.

[4] V. W. S. Chan, "Optical satellite networks," *J. Lightw. Technol.*, vol. 21, no. 11, pp. 2811–2827, Nov. 2003.

[5] L. Qu, G. Xu, Z. Zeng, N. Zhang, and Q. Zhang, "UAV-assisted RF/FSO relay system for space-air-ground integrated network: A performance analysis," *IEEE Trans. Wireless Commun.*, vol. 21, no. 8, pp. 6211–6225, Aug. 2022.

[6] N. Karafolas and S. Baroni, "Optical satellite networks," *J. Lightw. Technol.*, vol. 18, no. 12, pp. 1792–1806, 2000.

[7] S. Baroni and P. Bayvel, "Wavelength requirements in arbitrarily connected wavelength-routed optical networks," *J. Lightw. Technol.*, vol. 15, no. 2, pp. 242–251, Feb. 1997.

[8] S. Xue and C. Suzhi, "Wavelength routing assignment of optical networks on two typical LEO satellite constellations," in *Proc. Asia Commun. Photon. Conf.*, 2018, pp. 1–3, Paper. M1D.5.

[9] Z. Liu, W. Guo, C. Deng, W. Hu, and Y. Zhao, "Perfect match model-based link assignment to design topology for satellite constellation system," *Int. J. Satell. Commun. Netw.*, vol. 34, no. 2, pp. 263–276, 2016.

[10] X. Sun and S. Cao, "A routing and wavelength assignment algorithm based on two types of LEO constellations in optical satellite networks," *J. Lightw. Technol.*, vol. 38, no. 8, pp. 2106–2113, 2020.

[11] X. Liu, L. Yang, Q. Chen, J. Guo, S. Wu, and X. Chen, "An analytic method of wavelength requirements in dynamic optical satellite networks," *IEEE Commun. Lett.*, vol. 24, no. 11, pp. 2569–2573, Nov. 2020.

[12] Y. Zhu, M. Sheng, J. Li, and R. Liu, "Performance analysis of intermittent satellite link with time-limited queuing model," *IEEE Commun. Lett.*, vol. 22, no. 11, pp. 2282–2285, Nov. 2018.

[13] N. J. H. Marcano, L. Diez, R. A. Calvo, and R. H. Jacobsen, "On the queuing delay of time-varying channels in Low Earth Orbit satellite constellations," *IEEE Access*, vol. 9, pp. 87378–87390, 2021.

[14] H. Li et al., "Queue state based dynamical routing for non-geostationary satellite networks," in *Proc. IEEE 32nd Int. Conf. Adv. Inf. Netw. Appl.*, 2018, pp. 1–8.

[15] L. Tan, Y. Liu, and J. Ma, "Analysis of queuing delay in optical space network on LEO satellite constellations," *Optik*, vol. 125, no. 3, pp. 1154–1157, 2014.

[16] J. G. Walker, "Satellite constellations," *J. Brit. Interplanetary Soc.*, vol. 37, 1984, Art. no. 559.

[17] Q. Yang, L. Tan, and J. Ma, "Analysis of crosstalk in optical satellite networks with wavelength division multiplexing architectures," *J. Lightw. Technol.*, vol. 28, no. 6, pp. 931–938, Mar. 2010.

[18] L. Tan, Q. Yang, J. Ma, and S. Jiang, "Wavelength dimensioning of optical transport networks over nongeosychronous satellite constellations," *J. Opt. Commun. Netw.*, vol. 2, no. 4, pp. 166–174, 2010.

[19] Q. Yang, L. Tan, J. Ma, and S. Jiang, "An analytic method of dimensioning required wavelengths for optical WDM satellite networks," *IEEE Commun. Lett.*, vol. 15, no. 2, pp. 247–249, Feb. 2011.